Characterization of urban amine-containing particles in Southwestern China: seasonal variation, source, and processing

Yang Chen [1,2*], Mi Tian[1], Ru-jin Huang[2,6], Guangming Shi[4], Huanbo Wang[1], Chao Peng[1], Junji Cao[2,6], Qiyuan Wang[2], Shumin Zhang[3], Dongmei Guo[3], Leiming Zhang[5], and Fumo Yang[4,1] *

[1]Research Center for Atmospheric Environment, Chongqing Institute of Green and Intelligent Technology, Chinese Academy of Sciences, Chongqing 400714, China.

[2]Key Lab of Aerosol Chemistry & Physics, State Key Laboratory of Loess and Quaternary Geology, Institute of Earth Environment, Chinese Academy of Sciences, Xi'an 710061, China.

[3]School of Basic Medical Sciences, North Sichuan Medical College, Nanchong 637000, Sichuan, China.

[4] National Engineering Research Center for Flue Gas Desulfurization, Department of Environmental Science and Engineering, Sichuan University, Chengdu 610065, China

[5]Air Quality Research Division, Science and Technology Branch, Environment and Climate Change Canada, Toronto M3H 5T4, Canada

[6]Center for Excellence in Quaternary Science and Global Change, Chinese Academy of Sciences, Xi'an 710061, China.

Correspondence to: Yang Chen (chenyang@cigit.ac.cn); Fumo Yang (fmyang@scu.edu.cn)

Keyword: single particle; amine; urban environment, processing

Abstract

Amine-containing particles were characterized in an urban area of Chongqing during both summer and winter using a single particle aerosol mass spectrometer (SPAMS). Among the collected particles, 12.7% were amine-containing in winter and 8.3% in summer. Amines were internally mixed with elemental carbon (EC), organic carbon (OC), sulfate, and nitrate. Diethylamine (DEA) was the most abundant among amine-containing particles. Wintertime amine-containing particles were mainly from the northwest direction where a forest park was located; in summer, they were from the northwest and southwest (traffic hub) directions. These origins suggest that vegetation and traffic were the primary sources of particulate amines. The average relative peak area of DEA depended strongly on humidity, indicating that the enhancement of DEA was possibly due to increasing aerosol water content and aerosol acidity. Using an adaptive resonance theory neural network (ART-2a) algorithm, four major types of amine-containing particles were clustered including amine-organic-carbon (A-OC), A-OCEC, DEA-OC, and A-OCEC-aged. The identified particle types implied that amines were taken up by particles produced from traffic and biomass burning. Knowledge gained in this study is useful to understand the atmospheric processing, origin, and sources of amine-containing particles in the urban area of Chongqing.

1. Introduction

Amines are ubiquitous in the atmosphere and have both natural (ocean, biomass burning, and vegetation) and anthropogenic (animal husbandry, industry, combustion, and traffic) emission sources (Ge et al., 2011a). Trimethylamine (TMA) is one of the most abundant amines with an estimated global emission flux of 170Gg $year^{-1}$ (Ge et al., 2011a). Gaseous amines compete with ammonia in acid-base reactions, participate in gas-particle partitioning, and contribute to wet and dry deposition (Angelino et al., 2001; Monks, 2005; Gómez Alvarez et al., 2007; De Haan et al., 2011; Huang et al., 2012; You et al., 2014). Gaseous amines also play an essential role in new particle formation via enhancing the ternary nucleation of H_2SO_4-H_2O clusters in remote areas (Bzdek et al., 2012; Kirkby et al., 2011). In polluted areas, H_2SO_4-diethylamine (DMA)-water clusters were important during the new particle formation events (Yao et al., 2018). Amines are also essential in the growth of ambient particles. For example, particulate aminium salts, which were produced via amine-acid neutralization, tended to prevent the coagulation between pre-existing particles leading to increased particle number concentrations (Wang et al., 2010; Smith et al., 2010). Moreover, the enrichment of TMA had been observed in cloud and fog processing (Zhang et al., 2012; Rehbein et al., 2011). Characterization of amine-containing particles is important to evaluate their processing and impact.

Single particle mass spectrometers (SPMS), such as aerosol time-of-flight mass spectrometer (ATOFMS) and Single Particle Aerosol Mass Spectrometer (SPAMS), have been widely used in real-time measurements of amine-containing particles for chemical composition and mixing state (Li et al., 2017). SPAMS is different from the Aerodyne soot-particle aerosol mass spectrometer (SP-AMS), which is a type of

aerosol mass spectrometer (AMS) for detecting black carbon, sulfate, nitrate, ammonium, chloride, and organics (Onasch et al., 2012; Wang et al., 2016). The chemical composition and mixing state of TMA-containing particles have been reported worldwide, such as in California, USA (Denkenberger et al., 2007; Qin et al., 2012)); Ontario, Canada (Tan et al., 2002; Rehbein et al., 2011); Mexico City (Moffet et al., 2008)); European cities (Barcelona, Cork, Zurich, Paris, Dunkirk and Corsica (Healy et al., 2015; Dall'Osto et al., 2016)), and Chinese cities such as Guangzhou, Shanghai and Xi'an (Zhang et al., 2012; Chen et al., 2016; Huang et al., 2012). In the five European cities such as Cork, Paris, Dunkirk, Corsica, and Zurich, amines were found internally mixed with sulfate and nitrate; but in Corsica, amines were internally mixed with methanesulfonate (Healy et al., 2015). In Barcelona, five unique types of amine-containing particles were observed, including *amine-POA58* (composed of amines, sulfate, and nitrate), amine-*EST84*(environment tobacco smoke), *amine-SOA59* (composed of TMA and organics), *amine-SOA114*, and organic nitrogen amines (Dall'Osto et al., 2016; Dall'Osto et al., 2013). In a rural area site in the Pearl River Delta (China), the marker ion, $(C_2H_5)_2NH_2^+$, was the most abundant (90% and 86% of amine-containing particles in summer and winter) (Cheng et al., 2018). In Guangzhou, TMA-containing particles were important, taking up to 7% in number fraction during clear days and 35% during fog events (Zhang et al., 2012). In previous studies, reported high RH conditions and fog processing were favorable for the enhancement of trimethylamine in the particle phase. Zhang et al. found that, during fog events, the number fraction of TMA-containing particles took up to 35%; in the size range of 0.5-2.0 μm, the fraction accounted up to 60% (Zhang et al., 2012). Thus the location-specific studies in the varied environments are still necessary.

The knowledge of amine-containing particles is limited in southwestern China. In this region, Chongqing is a megacity with a population of 8.23 million. The city is subtropical, industrial, and polluted (Chen et al., 2017; Tao et al., 2017). Fog events frequently occurred in this area, and hence, it is known as the "fog city" in China. The effect of high relative humidity (RH) on the processing of amine-containing particles needs investigation. This study aims to characterize the amine-containing particles, including chemical composition, mixing state, atmospheric processing, and source in Chongqing during winter and summer.

2. Methods

2.1 Sampling site

Ambient single particles were collected at an urban air quality supersite from 07/05/2016 to 08/14/2016 (referred to as a summer season) and from 01/21/2016 to 02/25/2016 (referred to as a winter season). The supersite has been described in our previous studies (Chen et al., 2017). Briefly, the supersite is located on the rooftop of a commercial office building (106.51ºE, 29.62ºN) at a height of 30 m above the ground (Figure S1). The building is surrounded by business and residential communities and is 15 km from the city center. A 3 km^2 forest park is located northwest of the sampling site and a traffic hub in the southwest.

2.2 Instrumentation

A SPAMS (Hexin Inc. Guangzhou, China, model 0515) was deployed for single particle sampling, and the technical description of SPAMS is available in the literature (Li et al., 2011; Chen et al., 2017). Briefly, after passing through a diffusive dryer, particles in a size range of 0.1−2.0 μm are sampled via an aerodynamic lens and form

a particle beam. Particles in the beam come across two pre-positioned laser beams (Nd: YAG, 532 nm) one-by-one, and the vacuum aerodynamic diameter (D_{va}) of each particle is determined via its time-of-flight. Particles are ionized using an Nd: YAG laser operating at a wavelength of 266 nm. The ions are analyzed using a bipolar time-of-flight mass spectrometer. Due to the limitation of SPAMS, quantification of particulate amines was not attempted.

2.3 Data analysis

The SPAMS data were imported into the YAADA toolkit (Software Toolkit to Analyze Single-Particle Mass Spectral Data, v 2.11) to form a single particle dataset. The query was conducted using the marker ions of amines.: *m*/*z* 59 $[(CH_3)_3N]^+$ (TMA), 74 $[(C_2H_5)_2NH_2]^+$ (diethylamine, DEA), 86 $[(C_2H_5)_2NCH_2]^+$ or $[C_3H_7NHC_2H_4]^+$ (DEA or DPA), 101 $[(C_2H_5)_3N]^+$ (TEA), 102 $[(C_3H_7)_2NH_2]^+$ (DPA), 114 $[(C_3H_7)_2NCH_2]^+$ (DPA), and 143 $[(C_3H_7)_3N]^+$(TPA) (Healy et al., 2015). Firstly, *m*/*z* 59 was used for querying the TMA-containing particles; *m*/*z* 74 for the DEA-containing particles and *m*/*z* 86 for TEA-containing particles, and so on. The query strategy resulted in duplicate particles in the result when various amines co-existed in one single amine-containing particle. After the duplicate particles were removed from the multiple query results described above, all amine-containing particles were combined into an amine-containing particle cluster. Various amines could be both internally and externally mixed in these particle clusters.

An adaptive resonance theory based neural network algorithm (ART-2a) was applied to cluster the amine-containing particle types using a vigilance factor of 0.70, a learning rate of 0.05, and 20 iterations (Song et al., 1999). This procedure produced 67 clusters in summer and 75 clusters in winter; many of these clusters exhibited identical mass

spectra with slight differences in specific ion intensities. A well-established combining strategy, on the basis of similar mass spectra, temporal trends, and size distribution, was adopted to merge these particle clusters into the finalized particle types (Dallosto and Harrison, 2006). In addition, the relative peak area (RPA) is defined as the peak area of each *m*/*z* divided by the total dual-ion mass spectral peak areas of each particle (Healy et al., 2013). To calculate the overall RPA of amines, the relative peak area of amines in each particle were extracted and summed up.

3. Results and discussion

3.1 Single particle chemical composition and seasonal variation

The percentage of amine-containing particles was 12.7% in the winter SPAMS dataset and 8.3% in the summer dataset. The DEA-containing particles were dominant, accounting for 70% and 78% of all amine-containing particles in winter and summer, respectively; while TMA-containing particles were minor, accounting for up to 7% in winter and 3% in summer among all the amine-containing particles. The average mass spectra of DEA-, DPA, and TMA-containing particles are provided in Figure S2, and these spectra showed strong homogeneity. The determination coefficient (R^2) between DEA- and DPA- containing particles was 0.98, and R^2 between DEA- and TMA-containing particles was 0.83.

Figure 1 shows the digital mass spectra of amine-containing particles in two seasons. In each spectrum, the ion height indicates its fraction in the amine-containing particle dataset, and the stacked color map shows the corresponding ion intensity ranges. The assignment of ions is shown in Table S1. In both seasons, the dominant ions were K^+ (*m*/*z* 39 and 41), amines (*m*/*z* 59, 74, and 86), and organics (*m*/*z* 43, 51, 63, and 77). The

mixing ratios of ammonium (NH_4^+, *m*/*z* 18) and polycyclic aromatic hydrocarbons (e.g., *m*/*z* 116 ($[C_9H_8]^+$), 129 ($[C_{10}H_9]^+$), 140 ($[C_{11}H_8]^+$), and 153 ($[C_{12}H_9]^+$)) were higher in winter than in summer. The strong signal of NH_4^+ was possibly due to the lower temperature (8°C) in winter than in summer (31°C). The mixing ratios of *m*/*z* 59 were 45% and 44% during summer and winter, respectively.

In the negative mass spectra of two seasons (Figures 1(b) and 1(d)), the dominant ions were CN^- (*m*/*z* −26), CNO^- (*m*/*z* −42), nitrate (*m*/*z* −46 and −62), phosphate (−79), and sulfate (*m*/*z* −80 and −97). Primary species, such as CN^- and CNO^- were commonly from biomass burning (BB) and organonitrogen (Pratt et al., 2011). Levoglucosan markers from BB, such as −45, −59, and –71 were also detected. Dust markers, such as $[SiO_2]^-$ (*m*/*z* –60), $[^{28}SiO_3]^-$ or $[AlO_2(OH)]^-$ (–76), and $[PO_3]^-$, were also detected during summertime, suggesting the influence of dust particles.

Prior to comparison, the ion peak was normalized using the method developed by Qin et al. (2012). Briefly, the peak area of each m/z was divided by the total mass spectral peak area matrix. The normalized ion intensity of the wintertime particles was subtracted from that of the summertime particles. A positive value indicates the normalized ion intensity was greater in the summer, whereas a negative value indicates that the normalized ion intensity was greater in the winter. As shown in Figure S3, Ca^+ (*m*/*z* 40) and Fe^+ (*m*/*z* 56) were more prevalent during summer. Organic species, such as $C_2H_3^+$ (*m*/*z* 27), $C_4H_3^+$ (*m*/*z* 51), $C_5H_3^+$ (*m*/*z* 63), and $C_6H_5^+$ (*m*/*z* 77) typically from aromatic hydrocarbons, were also more abundant in summer. During wintertime, signals of sulfate (*m*/*z* −97), NO_3^- (*m*/*z* –62), NH_4^+ (*m*/*z* 18), and K^+ (*m*/*z* 39) were more prominent than in summer, suggesting that the wintertime particles contained more secondary species than those in summer.

The unscaled size distribution of amine-containing particles also showed strong seasonal variations (Figure S4). Generally, amine-containing particles had monomodal size distributions in the droplet mode; and the distributions peaked at a larger D_{va} in summer than winter. For example, DEA-containing particles peaked at 0.6 μm in winter and 0.8 μm in summer, and DPA-containing particles at 0.7 μm in winter and 0.9 μm in summer. The size distributions of the major amine-containing particles suggested that these particles had undergone substantial aging processes.

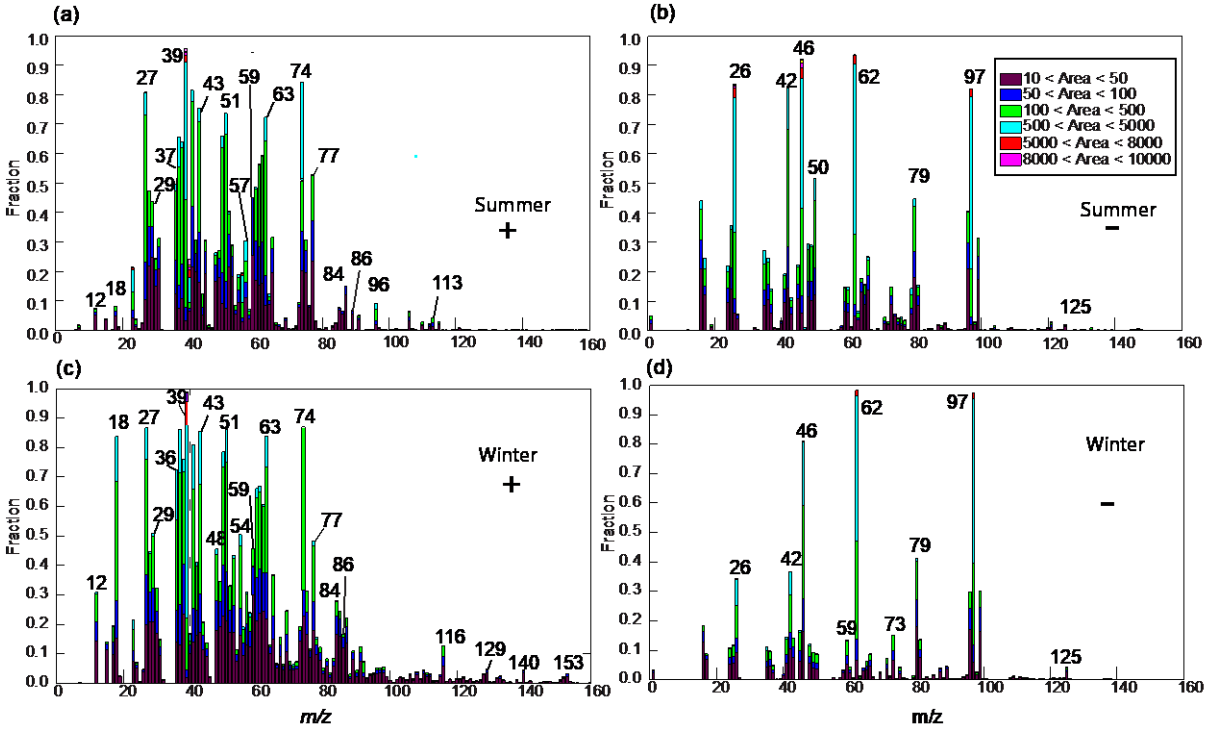

Figure 1. (a) and (c): the positive digital mass spectrum of amine-containing particles during summer and wintertime, respectively; (b) and (d): the negative digital mass spectrum during summer and wintertime, respectively. The ion height indicates its fraction in the amine-containing particle dataset, and the stacked color map indicates the ion peak area range.

3.2 Temporal trend, diurnal pattern, and origin of amine-containing particles

Figure 2 shows the temporal tends of RH, temperature, number count, and the peak area of amine-containing particles. The winter temperature was lower (8.0±4.0ºC) than summer (31±4ºC), and RH in the winter was slightly higher (70±14% versus 64±16%) (Table 1). Stagnant air conditions occurred in both seasons due to the low wind speeds (Huang et al., 2017), and the winter wind speed was lower than in summer. The hourly count of amine-containing particles was typically ten times higher in winter than summer.

In winter, a good correlation existed between the temporal trends of hourly number count and peak area of DEA-containing particles ($R^2 = 0.86$). The corresponding R^2 in wintertime DPA-containing particles was 0.88. No such correlation for TMA-containing particles was observed in winter ($R^2 = 0.22$) or summer (Figure 2). The hourly counts of DEA- and DPA-containing particles were well correlated in both summer ($R^2 = 0.63$) and winter ($R^2 = 0.87$), but a weak correlation ($R^2 = 0.25$) existed between DEA- and TMA-containing particles. These results suggest DEA- and DPA-containing particles were possibly from the same sources.

Table 1. Meteorological factors and particle counts in summer and winter.

	Winter	Summer
Temperature (ºC)	8 ±4	31±4
Relative humidity (%)	70±14	64±16
Wind Speed	1.2±0.7	1.5±1.0
Amine-particle Count (# h^{-1})	587±384	47±26

DEA- and DPA-containing particles remained at low levels from 1/20/2016 to 01/26/2016 and averaged at 109 and 26 count h^{-1}, respectively. During this period, wind speed was relatively high, commonly above 1.5 ms^{-1}. TMA-, DEA-, and DPA-containing particles started accumulating after 01/26/2016 when wind speed was low (0.8 ms^{-1}) and wind direction from the northwest. After 02/03/2016, DEA- and DPA-containing particles showed regular diurnal patterns with high levels of hourly count during daytime on most days and minimum levels at 15:00. A similar diurnal pattern was also observed for DPA-containing particles during wintertime (Figures 3). TMA-containing particles presented a complex diurnal profile with peaks in the early morning (4:00), at noon (12:00) and in the afternoon (18:00). The chemical composition and diurnal pattern of TMA-containing particles were strongly connected to traffic emissions.

Wind direction and number count of amine-containing particles were analyzed together using bivariate polar plots (Figure 4). During wintertime, the dominant direction for amine-containing particles was from the northwest where a forest park was located. After being emitted from vegetation (plants, grass, and trees) (Ge et al., 2011a), DEA could partition to the pre-existing particles before arriving at the sampling site. The transport of these particles to the sampling site caused the elevation in the morning. Based on the excellent correlation between DEA- and DPA-containing particles, DPA-containing particles could also be from vegetation. It can be concluded that the major source of amines in DEA- and DPA-containing particles was vegetation from the northwest.

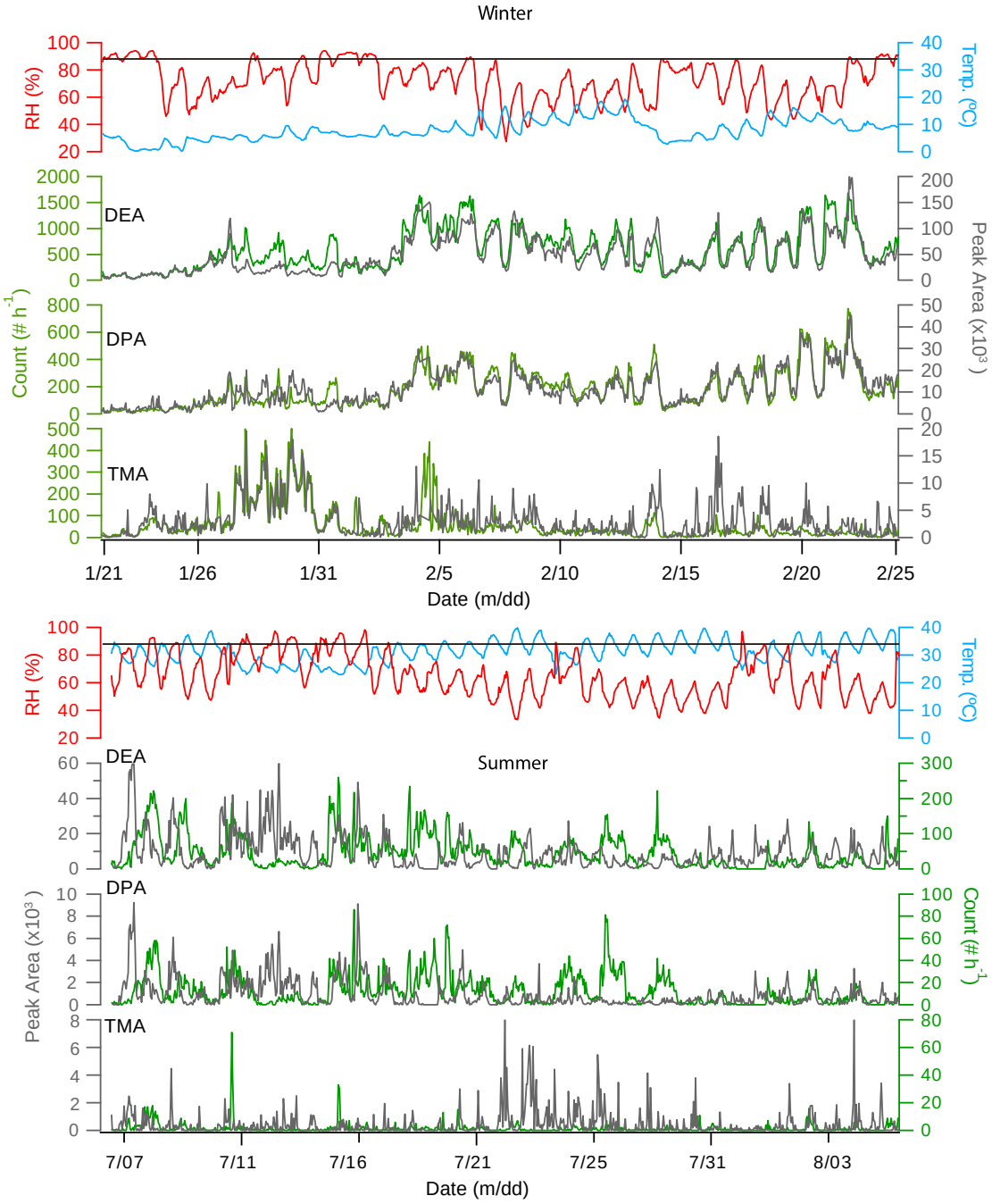

239

240 Figure 2. Temporal trends of relative humidity (RH), temperature (Temp.), hourly peak
241 area (dark gray), and particle count (green) of DEA (*m/z* 74), DPA (*m/z* 86), and TMA
242 (*m/z* 59) -containing particles in winter (top panel) and summer (bottom panel). The
243 black lines in the two panels indicate RH of 90%.

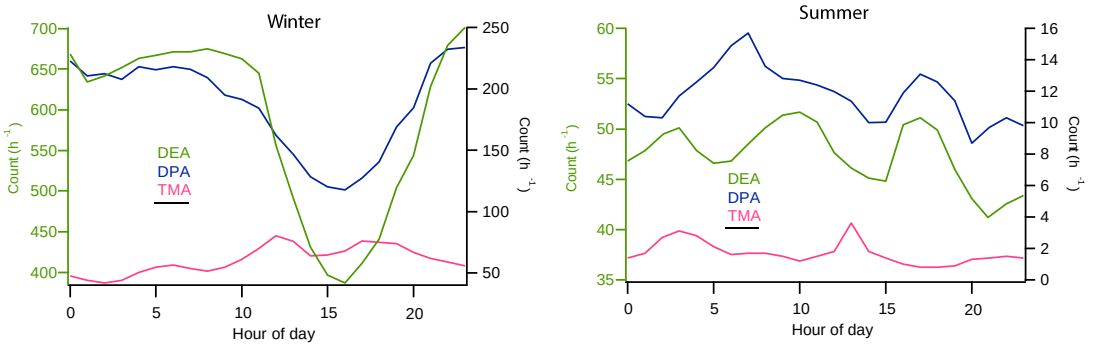

244

245 Figure 3. Diurnal profiles of amine-containing particles during both winter (left panel)
246 and summer (right panel). The green left axis in each panel indicates the average
247 number count of DEA-containing particles, while the right-axis represents the number
248 count of both DPA- and TMA-containing particles.

249 During summer, the amine particles appeared in several episodes; each episode lasted
250 for 1~3 days. In these episodes, DPA-containing particles had two rush-hour peaks
251 (7:00 and 17:00), likely from traffic (Dall'Osto et al., 2016). Besides traffic, vegetation
252 is also a source of DPA-containing particles (from the southwest, Figure 4e). The DPA-
253 containing particles peaked 0.84 μm, suggesting that they were not freshly-emitted and
254 had undergone substantial aging processes. Moreover, as shown in Figure S2, the mass
255 spectra of the amines were present with aromatic hydrocarbon fragments, such as $C_4H_3^+$
256 (*m*/*z* 51), $C_5H_3^+$ (*m*/*z* 63), $C_6H_5^+$ (*m*/*z* 77), and $C_9H_8^+$ (*m*/*z* 116), as well as with alkanes
257 fragments such as $C_4H_7^+$ (*m*/*z* 55), $C_4H_9^+$ (*m*/*z* 57), and $C_5H_9^+$ (*m*/*z* 69). The chemical
258 composition of DPA-containing particles contained markers associated with traffic
259 emissions. Similar amine-containing particle type has been reported in the literature
260 (Dall'Osto et al., 2016).

261 In summer, DEA-containing particles had a diurnal pattern of three peaks appearing at
262 3:00, 9:00 and 17:00. TMA-containing particles had an early morning (4:00) and a noon
263 peak (12:00). The morning peaks of DEA- and TMA-containing particles could be due

to the local traffic emissions; specifically, heavy-duty vehicles were only allowed to enter the urban area between 00:00 and 6:00 (Chen et al., 2017). The polar plots showed that DEA-containing particles were from the northwest and southwest, passing through the forest park and traffic hub, respectively. This scenario seemed to be inconsistent with the wintertime results because of the limited traffic contributions to particle levels in winter. In addition, due to the competition between vegetation and traffic in summer, the number count and peak area of all three amine-containing particles were poorly correlated with each other.

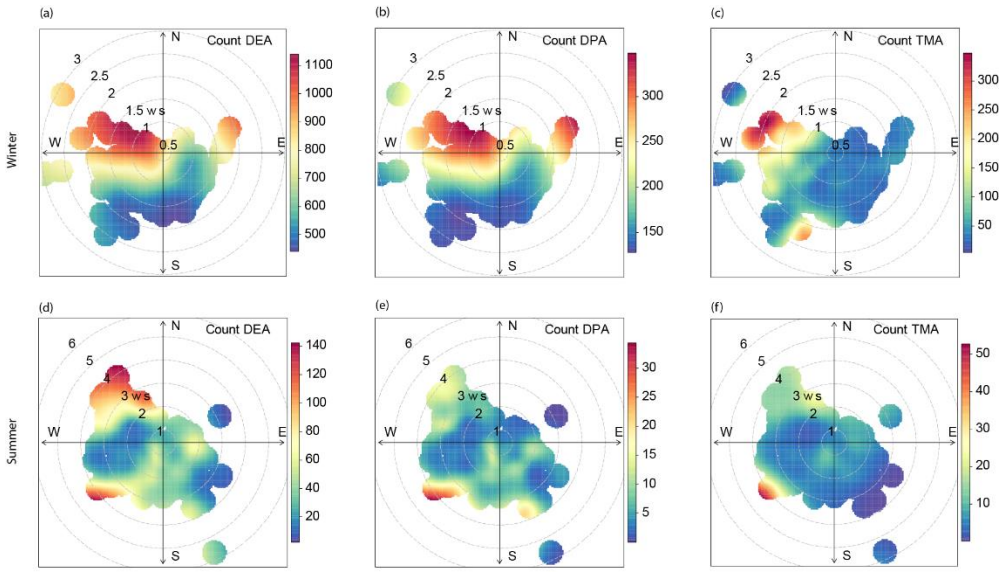

Figure 4. Polar plots of amine-containing particles during winter- and summertime. The axes in each figure indicate hourly count of each particle type and the colors within the circles represent wind speed (ws)

3.3 Effect of RH on the enrichment of DEA-containing particles

DEA-containing particles were predominant in both winter and summer, providing a unique opportunity for investigating DEA processing. Indeed, the effect of RH on aerosol chemical processing should be treated cautiously and the influences of wind

speed, wind direction, temperature, and planetary boundary layer reduction should be removed. As described above, the average wind speed in both winter and summer was 1.2 ms^{-1} and 1.5 ms^{-1}, respectively. In these stagnant air conditions, the sampled particles were generally local. Temperature could influence the gas-particle phase partitioning. Assuming the Henry's Law constants (K_H) and the enthalpy change $\Delta_r H_o(K_H)$ of DEA are constant, a variation of 10ºC in both summer and winter has negligible influence on the partitioning of amines from the gas phase to the particle phase, according to the Clapeyron equation (Ge et al., 2011b). In addition, the shift in planetary boundary layer (PBL) height could affect the number count and concentration of PM. Using the temporal trends of RPA, the influence of PBL height can be removed because it only shows the relative changes between different species which are all simultaneously influenced by the shift in the PBL height.

Box plots of DEA relative peak area under different RH are shown in Figure 5. In winter, the median RPA of amine-containing particles increased by two times when RH increased from 35% to 95%. Meanwhile, the fraction of DEA-containing particles increased from 4.0% to 16.6%. In summer, the average RPA of DEA increased by three times (from 0.25 to 0.75) and the fraction of DEA-containing particles ramped from 3.8% to 12.1% when RH increased from 60% to 90%. These results suggest that RH is important to the enrichment of DEA in the particle phase. When DEA reacts with HCl, H_2SO_4, and HNO_3, it tends to form aminium salts, which are soluble in aerosol water. Along with the influence of aerosol water content, Ge et al. (2011a) also proposed that strong aerosol acidity could also enhance the partitioning of DEA in the aqueous phase. As particles are dried in the SPAMS, the amount of aerosol water content and pH were unavailable. The values of the anion/ cation ratio ((sulfate +nitrate)/ammonium, Yao et al. (2011) were in a range of 20-150 suggesting that the particles might have been acidic

which favors the dissolution of DEA. Overall, these results implied that high RH conditions in Chongqing was favorable for particle uptake of DEA, and the resulting formation of aminium salts stabilized pre-existing particles; thus, increased their number concentrations.

Rehbein et al. (2011) and Zhang et al. (2012) observed direct links between fog processing and enhancement of TMA-containing particles. High RH conditions were favorable for TMA entering the particle phase via gas -particle partitioning (Rehbein et al., 2011; Zhang et al., 2012). Ge et al. (2011b) argued that TMA in the aerosol phase was in the form of free base, e.g., amine, not aminium salt; TMA could be dissolved in the aerosol water; the formation of TMA-HSO_4 salt was possible, but the formation of TMA-NO_3 and TMA-Cl was impossible due to the competition with ammonia. Thus, TMA could enter the aerosol phase by gas-aqueous partitioning, or in the form of TMA-HSO_4 salt. The mechanism of DEA entering the aerosol phase might be different from TMA. DEA salts were favorable for forming in aerosol phase (Ge et al., 2011b). Besides, Pankow (2015) proposed that the absorptive uptake of atmospheric amines could also be possible on organic aerosols. In the context of single particle mixing state, the amine-containing particles were internally mixed with hygroscopic species, e.g., sulfate, nitrate, POA species ($C_xH_y^+$, see section 3.4), and SOA species (oxalate, $C_2H_3O^+$). Therefore, the mixing state of amine-containing particles was also favorable for the uptake of amines via different pathways: the aqueous dissolution of aminium salts and the absorptive uptake on OA.

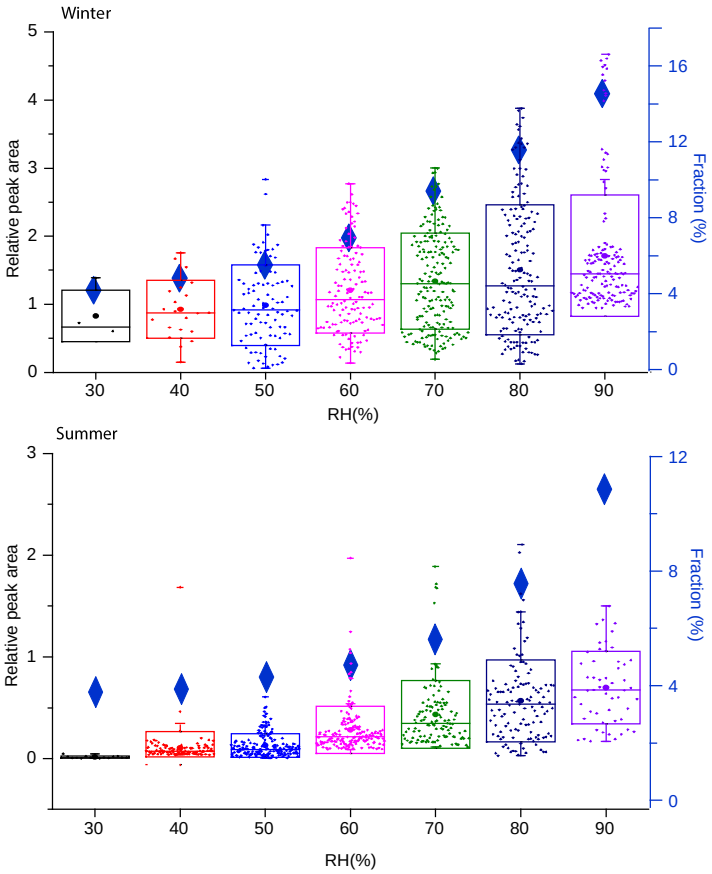

326

327 Figure 5. Box plots of the hourly relative peak area of DEA under different RH
328 conditions in winter (top panel) and summer (bottom panel). The boxes indicate the
329 25th and 75th percentiles; the dots indicate mean value with each data point representing
330 a datum of RPA in an hour size bin. Right axis in each panel and the blue diamonds
331 show the average number fraction of amine-containing particles among the whole
332 SPAMS dataset.

333 **3.4 Particle types of amine-containing particles**

334 As shown in Figure 6, four amine-containing particle types were resolved, including
335 amine-OC (A-OC, 41%), A-ECOC (39%), DEA-OC (11%), and A-ECOC-aged (9%).
336 All of these particle types had strong signals of amines, and the amines were internally
337 mixed with sulfate, nitrate, elemental carbon, and organics.

In the A-OC particles, amines were mixed with aromatic hydrocarbon fragments, such as $C_4H_3^+$ (*m*/*z* 51), $C_5H_3^+$ (*m*/*z* 63), $C_6H_5^+$ (*m*/*z* 77), and $C_9H_8^+$ (*m*/*z* 116), as well as with alkanes fragments such as $C_4H_7^+$ (*m*/*z* 55), $C_4H_9^+$ (*m*/*z* 57), and $C_5H_9^+$ (*m*/*z* 69). In the negative mass spectrum of A-OC, strong signals from CN^- (*m*/*z* −26) and CNO^- (*m*/*z* −42) were typically primary species, along with levoglucosan (Silva et al., 1999). The amine fragments, such as TMA (*m*/*z* 59), DEA (*m*/*z* 74), and DPA (*m*/*z* 86), were very abundant in this particle type (76%, 95%, and 88%, respectively). The parent particles of A-OC were a kind of OC particles from biomass burning; then they mixed with amines via uptake. Amines could enter the A-OC particle type via dissolution in the aerosol water content or uptake due to absorptive uptake on the organic aerosol (Pankow, 2015).

In A-ECOC mass spectra, strong signals of amines (*m*/*z* 59 and 74), along with the major aromatic hydrocarbon fragments and EC components (i.e., *m*/*z* 36, 48, 60) were detected. In the negative mass spectra, nitrate and sulfate were also dominant. The A-ECOC-aged particle type had a similar chemical composition to A-ECOC (R^2 =0.53) but with weaker relative intensities of $C_xH_y^+$ and amine ions, suggesting it could be more secondary.

In the positive mass spectra of DEA-OC, DEA fragment (*m*/*z* 74) was dominant and present with organic fragments described above. The secondary organic marker ions, such as *m*/*z* 43 ($[C_2H_3O]^+$) and –89 (oxalic acid), were found in the mass spectra. Besides, DEA-OC was not sensitive to wind speed (R^2 =0.18), implying they were local.

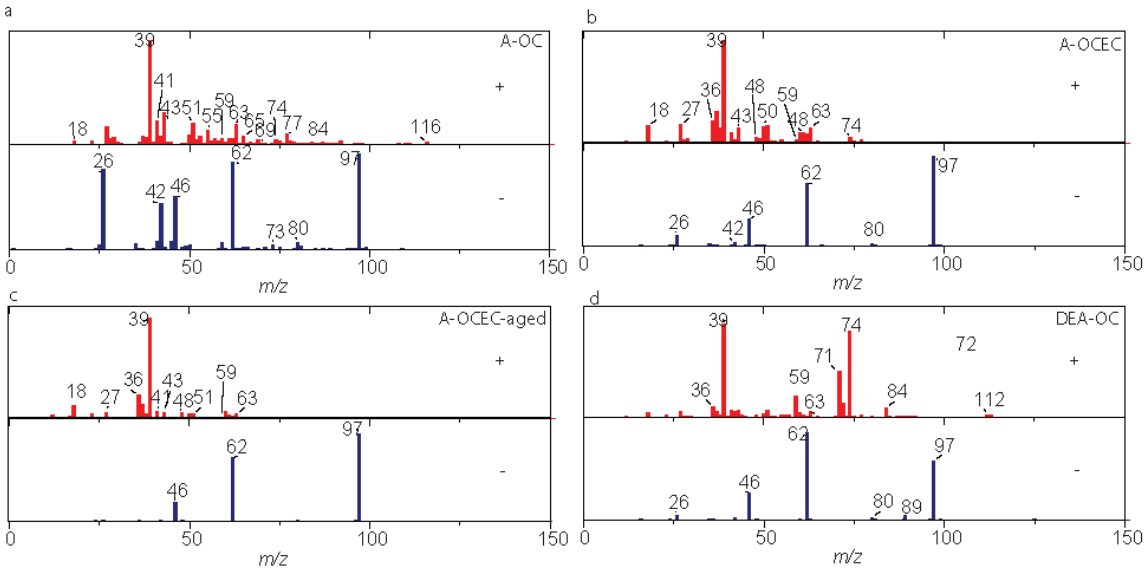

359

360 Figure 6. Average mass spectra of major particle types clustered from amine-containing
361 particles.

362 The summertime amine-containing particles were similar to the particle types during
363 winter (all R^2 >0.7), except a Ca-rich particle type was also resolved (Figure S5). A-
364 Ca-OC particle type was mainly composed of calcium (Ca^+ and CaO^+), sodium (*m*/*z*
365 23), potassium (*m*/*z* 39), TMA (*m*/*z* 59), sulfate, nitrate, and phosphate. An ion signal
366 of zinc (m/z 64) was observed in the positive mass spectrum. Zn is a marker for tire
367 wear on roads (Grigoratos and Martini, 2015; Thorpe and Harrison, 2008). The A-Ca-
368 OC particle type was possibly from traffic activities (Chen et al., 2017).

369 The amine-containing particle types reported in this study were different from those in
370 literature. Cheng et al. (2018) reported that *m*/*z* 74 amine-containing particles were most
371 abundant in the Pearl River Delta, China, but the chemical composition and mixing
372 state of amine particles were different from this study. For example, the mixing ratio of
373 DPA was much stronger (~0.2) in Guangdong than in Chongqing (<0.1). In most related
374 studies, TMA-containing particles were dominant, while the present study showed

DEA-containing particles were dominant (Rehbein et al., 2011; Zhang et al., 2012; Healy et al., 2015; Dall'Osto et al., 2016).

4. Conclusions

Amine-containing particles were collected and analyzed during winter and summer in the urban area of Chongqing. Generally, amine-containing particles were more abundant in winter than in summer. DEA-containing particles (*m*/*z* 74) were the most important particle type during both summer and winter. Amines were internally mixed with EC components, organics, sulfate, and nitrate, suggesting particle aging was significant in both seasons. Amine-containing particles had monomodal size distributions in the droplet mode, and the distributions peaked at a larger D_{va} in summer than winter. DEA- and DPA-containing particles showed strong homogeneity, and good correlations between the hourly number count and peak area were observed during winter. The amine-containing particles were mostly from vegetation located southwest of the sampling area, and traffic sources in the northwest. An enrichment of DEA-containing particles under high RH conditions was revealed. Reduction of anthropogenic amines, such as DEA and TMA, would improve the air quality in this region, which can be achieved by decreasing the emissions of on-road fuel-powered automobiles.

Acknowledgments. Financial support from the National Key Research and Development Program of China (2018YFC0200403 and 2016YFC0200405), the Nature Science Foundation of China (Grant No. 41375123), and the Educational Commission of Sichuan Province of China（No. 15ZA0213） are acknowledged.

Author Contribution. CY and YF designed the experiments; TM, SG, PC, WH, and WQ carried them out; HR, CY, ZL, CJ, and GD analyzed the experiment data; CY prepared the manuscript with contributions from all co-authors.

References

Angelino, S., Suess, D. T., and Prather, K. A.: Formation of aerosol particles from reactions of secondary and tertiary alkylamines: characterization by aerosol time-of-flight mass spectrometry, Environ Sci Technol, 35, 3130-3138, 10.1021/es0015444, 2001.

Bzdek, B. R., Zordan, C. A., Pennington, M. R., Luther, G. W., 3rd, and Johnston, M. V.: Quantitative assessment of the sulfuric acid contribution to new particle growth, Environ Sci Technol, 46, 4365-4373, 10.1021/es204556c, 2012.

Chen, Y., Cao, J., Huang, R., Yang, F., Wang, Q., and Wang, Y.: Characterization, mixing state, and evolution of urban single particles in Xi'an (China) during wintertime haze days, Sci Total Environ, 573, 937-945, 10.1016/j.scitotenv.2016.08.151, 2016.

Chen, Y., Yang, F., Mi, T., Cao, J., Shi, G., Huang, R., Wang, H., Chen, J., Lou, S., and Wang, Q.: Characterizing the composition and evolution of and urban particles in Chongqing (China) during summertime, Atmos Res, 187, 84-94, 10.1016/j.atmosres.2016.12.005, 2017.

Cheng, C. L., Huang, Z. Z., Chan, C. K., Chu, Y. X., Li, M., Zhang, T., Ou, Y. B., Chen, D. H., Cheng, P., Li, L., Gao, W., Huang, Z. X., Huang, B., Fu, Z., and Zhou, Z.: Characteristics and mixing state of amine-containing particles at a rural site in the Pearl River Delta, China, Atmos Chem Phys, 18, 9147-9159, 10.5194/acp-18-9147-2018, 2018.

Dall'Osto, M., Querol, X., Alastuey, A., Minguillon, M. C., Alier, M., Amato, F., Brines, M., Cusack, M., Grimalt, J. O., Karanasiou, A., Moreno, T., Pandolfi, M., Pey, J., Reche, C., Ripoll, A., Tauler, R., Van Drooge, B. L., Viana, M., Harrison, R. M., Gietl, J., Beddows, D., Bloss, W., O'Dowd, C., Ceburnis, D., Martucci, G., Ng, N. L., Worsnop, D., Wenger, J., Mc Gillicuddy, E., Sodeau, J., Healy, R., Lucarelli, F., Nava, S., Jimenez, J. L., Gomez Moreno, F., Artinano, B., Prévôt, A. S. H., Pfaffenberger, L., Frey, S., Wilsenack, F., Casabona, D., Jiménez-Guerrero, P., Gross, D., and Cots, N.: Presenting SAPUSS: Solving Aerosol Problem by Using Synergistic Strategies in Barcelona, Spain, Atmos. Chem. Phys., 13, 8991-9019, 10.5194/acp-13-8991-2013, 2013.

Dall'Osto, M., Beddows, D. C. S., McGillicuddy, E. J., Esser-Gietl, J. K., Harrison, R. M., and Wenger, J. C.: On the simultaneous deployment of two single-particle mass spectrometers at an urban background and a roadside site during SAPUSS, Atmos Chem Phys, 16, 9693-9710, 10.5194/acp-16-9693-2016, 2016.

Dallosto, M., and Harrison, R.: Chemical characterisation of single airborne particles in Athens (Greece) by ATOFMS, Atmos Environ, 40, 7614-7631, 10.1016/j.atmosenv.2006.06.053, 2006.

De Haan, D. O., Hawkins, L. N., Kononenko, J. A., Turley, J. J., Corrigan, A. L., Tolbert, M. A., and Jimenez, J. L.: Formation of nitrogen-containing oligomers by methylglyoxal and amines in simulated evaporating cloud droplets, Environ Sci Technol, 45, 984-991, 10.1021/es102933x, 2011.

Denkenberger, K. A., Moffet, R. C., Holecek, J. C., Rebotier, T. P., and Prather, K. A.: Real-time, single-particle measurements of oligomers in aged ambient aerosol particles, Environ Sci Technol, 41, 5439-5446, 10.1021/es070329l, 2007.

Ge, X., Wexler, A. S., and Clegg, S. L.: Atmospheric amines – Part I. A review, Atmos Environ, 45, 524-546, 10.1016/j.atmosenv.2010.10.012, 2011a.

Ge, X., Wexler, A. S., and Clegg, S. L.: Atmospheric amines – Part II. Thermodynamic properties and gas/particle partitioning, Atmos Environ, 45, 561-577, 10.1016/j.atmosenv.2010.10.013, 2011b.

Gómez Alvarez, E., Viidanoja, J., Muñoz, A., Wirtz, K., and Hjorth, J.: Experimental Confirmation of the Dicarbonyl Route in the Photo-oxidation of Toluene and Benzene, Environ Sci Technol, 41, 8362-8369, 10.1021/es0713274, 2007.

Grigoratos, T., and Martini, G.: Brake wear particle emissions: a review, Environ Sci Pollut Res Int, 22, 2491-2504, 10.1007/s11356-014-3696-8, 2015.

Healy, R. M., Sciare, J., Poulain, L., Crippa, M., Wiedensohler, A., Prevot, A. S. H., Baltensperger, U., Sarda-Esteve, R., McGuire, M. L., Jeong, C. H., McGillicuddy, E., O'Connor, I. P., Sodeau, J. R., Evans, G. J., and Wenger, J. C.: Quantitative determination of carbonaceous particle mixing state in Paris using single-particle mass spectrometer and aerosol mass spectrometer measurements, Atmos Chem Phys, 13, 9479-9496, 10.5194/acp-13-9479-2013, 2013.

Healy, R. M., Evans, G. J., Murphy, M., Sierau, B., Arndt, J., McGillicuddy, E., O'Connor, I. P., Sodeau, J. R., and Wenger, J. C.: Single-particle speciation of alkylamines in ambient aerosol at five European sites, Anal Bioanal Chem, 407, 5899-5909, 10.1007/s00216-014-8092-1, 2015.

Huang, Q., Cai, X., Song, Y., and Zhu, T.: Air stagnation in China (1985–2014): climatological mean features and trends, Atmos. Chem. Phys., 17, 7793-7805, 10.5194/acp-17-7793-2017, 2017.

Huang, Y., Chen, H., Wang, L., Yang, X., and Chen, J.: Single particle analysis of amines in ambient aerosol in Shanghai, Environ Chem, 9, 202-210, 10.1071/en11145, 2012.

Kirkby, J., Curtius, J., Almeida, J., Dunne, E., Duplissy, J., Ehrhart, S., Franchin, A., Gagne, S., Ickes, L., Kurten, A., Kupc, A., Metzger, A., Riccobono, F., Rondo, L., Schobesberger, S., Tsagkogeorgas, G., Wimmer, D., Amorim, A., Bianchi, F., Breitenlechner, M., David, A., Dommen, J., Downard, A., Ehn, M., Flagan, R. C., Haider, S., Hansel, A., Hauser, D., Jud, W., Junninen, H., Kreissl, F., Kvashin, A., Laaksonen, A., Lehtipalo, K., Lima, J., Lovejoy, E. R., Makhmutov, V., Mathot, S., Mikkila, J., Minginette, P., Mogo, S., Nieminen, T., Onnela, A., Pereira, P., Petaja, T., Schnitzhofer, R., Seinfeld, J. H., Sipila, M., Stozhkov, Y., Stratmann, F., Tome, A., Vanhanen, J., Viisanen, Y., Vrtala, A., Wagner, P. E., Walther, H., Weingartner, E., Wex, H., Winkler, P. M., Carslaw, K. S., Worsnop, D. R., Baltensperger, U., and Kulmala, M.: Role of sulphuric acid, ammonia and galactic cosmic rays in atmospheric aerosol nucleation, Nature, 476, 429-433, 10.1038/nature10343, 2011.

Li, L., Huang, Z., Dong, J., Li, M., Gao, W., Nian, H., Fu, Z., Zhang, G., Bi, X., Cheng, P., and Zhou, Z.: Real time bipolar time-of-flight mass spectrometer for analyzing single aerosol particles, Int J Mass Spectrom, 303, 118-124, 10.1016/j.ijms.2011.01.017, 2011.

Li, Y. J., Sun, Y., Zhang, Q., Li, X., Li, M., Zhou, Z., and Chan, C. K.: Real-time chemical characterization of atmospheric particulate matter in China: A review, Atmos Environ, 2017.

Moffet, R. C., de Foy, B., Molina, L. T., Molina, M. J., and Prather, K. A.: Measurement of ambient aerosols in northern Mexico City by single particle mass spectrometry, Atmos. Chem. Phys., 8, 4499-4516, 10.5194/acp-8-4499-2008, 2008.

Monks, P. S.: Gas-phase radical chemistry in the troposphere, Chem Soc Rev, 34, 376-395, 10.1039/b307982c, 2005.

Onasch, T. B., Trimborn, a., Fortner, E. C., Jayne, J. T., Kok, G. L., Williams, L. R., Davidovits, P., and Worsnop, D. R.: Soot Particle Aerosol Mass Spectrometer: Development, Validation, and Initial Application, Aerosol Sci. Technol., 46, 804-817, 10.1080/02786826.2012.663948, 2012.

Pankow, J. F.: Phase considerations in the gas/particle partitioning of organic amines in the atmosphere, Atmos Environ, 122, 448-453, 10.1016/j.atmosenv.2015.09.056, 2015.

Pratt, K. A., Murphy, S. M., Subramanian, R., DeMott, P. J., Kok, G. L., Campos, T., Rogers, D. C., Prenni, A. J., Heymsfield, A. J., Seinfeld, J. H., and Prather, K. A.: Flight-based chemical characterization of biomass burning aerosols within two prescribed burn smoke plumes, Atmos Chem Phys, 11, 12549-12565, 10.5194/acp-11-12549-2011, 2011.

Qin, X., Pratt, K. A., Shields, L. G., Toner, S. M., and Prather, K. A.: Seasonal comparisons of single-particle chemical mixing state in Riverside, CA, Atmos Environ, 59, 587-596, 10.1016/j.atmosenv.2012.05.032, 2012.

Rehbein, P. J., Jeong, C. H., McGuire, M. L., Yao, X., Corbin, J. C., and Evans, G. J.: Cloud and fog processing enhanced gas-to-particle partitioning of trimethylamine, Environ Sci Technol, 45, 4346-4352, 10.1021/es1042113, 2011.

512 Silva, P. J., Liu, D.-Y., Noble, C. A., and Prather, K. A.: Size and Chemical
513 Characterization of Individual Particles Resulting from Biomass Burning of Local
514 Southern California Species, Environ Sci Technol, 33, 3068-3076, 10.1021/es980544p,
515 1999.

516 Smith, J. N., Barsanti, K. C., Friedli, H. R., Ehn, M., Kulmala, M., Collins, D. R.,
517 Scheckman, J. H., Williams, B. J., and McMurry, P. H.: Observations of aminium salts
518 in atmospheric nanoparticles and possible climatic implications, Proc Natl Acad Sci U
519 S A, 107, 6634-6639, 10.1073/pnas.0912127107, 2010.

520 Song, X. H., Hopke, P. K., Fergenson, D. P., and Prather, K. A.: Classification of single
521 particles analyzed by ATOFMS using an artificial neural network, ART-2A, Anal.
522 Chem., 71, 860-865, DOI 10.1021/ac9809682, 1999.

523 Tan, P. V., Evans, G. J., Tsai, J., Owega, S., Fila, M. S., Malpica, O., and Brook, J. R.:
524 On-line analysis of urban particulate matter focusing on elevated wintertime aerosol
525 concentrations, Environ Sci Technol, 36, 3512-3518, 10.1021/es011448i, 2002.

526 Tao, J., Zhang, L., Cao, J., and Zhang, R.: A review of current knowledge concerning
527 PM_{2. 5} chemical composition, aerosol optical properties and
528 their relationships across China, Atmos Chem Phys, 17, 9485-9518, 10.5194/acp-17-
529 9485-2017, 2017.

530 Thorpe, A., and Harrison, R. M.: Sources and properties of non-exhaust particulate
531 matter from road traffic: a review, Sci Total Environ, 400, 270-282,
532 10.1016/j.scitotenv.2008.06.007, 2008.

533 Wang, J. F., Ge, X. L., Chen, Y. F., Shen, Y. F., Zhang, Q., Sun, Y. L., Xu, J. Z., Ge,
534 S., Yu, H., and Chen, M. D.: Highly time-resolved urban aerosol characteristics during

springtime in Yangtze River Delta, China: insights from soot particle aerosol mass spectrometry, Atmos Chem Phys, 16, 9109-9127, 10.5194/acp-16-9109-2016, 2016.

Wang, L., Khalizov, A. F., Zheng, J., Xu, W., Ma, Y., Lal, V., and Zhang, R.: Atmospheric nanoparticles formed from heterogeneous reactions of organics, Nature Geoscience, 3, 238, 10.1038/ngeo778

https://www.nature.com/articles/ngeo778#supplementary-information, 2010.

Yao, L., Garmash, O., Bianchi, F., Zheng, J., Yan, C., Kontkanen, J., Junninen, H., Mazon, S. B., Ehn, M., Paasonen, P., Sipila, M., Wang, M., Wang, X., Xiao, S., Chen, H., Lu, Y., Zhang, B., Wang, D., Fu, Q., Geng, F., Li, L., Wang, H., Qiao, L., Yang, X., Chen, J., Kerminen, V. M., Petaja, T., Worsnop, D. R., Kulmala, M., and Wang, L.: Atmospheric new particle formation from sulfuric acid and amines in a Chinese megacity, Science, 361, 278-281, 10.1126/science.aao4839, 2018.

Yao, X., Rehbein, P. J. G., Lee, C. J., Evans, G. J., Corbin, J., and Jeong, C.-H.: A study on the extent of neutralization of sulphate aerosol through laboratory and field experiments using an ATOFMS and a GPIC, Atmos Environ, 45, 6251-6256, 10.1016/j.atmosenv.2011.06.061, 2011.

You, Y., Kanawade, V. P., de Gouw, J. A., Guenther, A. B., Madronich, S., Sierra-Hernández, M. R., Lawler, M., Smith, J. N., Takahama, S., Ruggeri, G., Koss, A., Olson, K., Baumann, K., Weber, R. J., Nenes, A., Guo, H., Edgerton, E. S., Porcelli, L., Brune, W. H., Goldstein, A. H., and Lee, S. H.: Atmospheric amines and ammonia measured with a chemical ionization mass spectrometer (CIMS), Atmos. Chem. Phys., 14, 12181-12194, 10.5194/acp-14-12181-2014, 2014.

Zhang, G., Bi, X., Chan, L. Y., Li, L., Wang, X., Feng, J., Sheng, G., Fu, J., Li, M., and Zhou, Z.: Enhanced trimethylamine-containing particles during fog events detected by

559 single particle aerosol mass spectrometry in urban Guangzhou, China, Atmos Environ,
560 55, 121-126, 10.1016/j.atmosenv.2012.03.038, 2012.

561